[8] D. J. Coleman and S. M. Sze, "A low noise metal-semiconductor-metal (MSM) microwave oscillator," *Bell Syst. Tech. J.*, vol. 50, pp. 1695–1699, May–June 1971.
[9] C. A. Lee and G. C. Dalman, "Local oscillator noise in a silicon Pt-n-p$^+$ microwave diode source," *Electron Lett.*, vol. 7, pp. 565–566, Sept. 1971.
[10] G. Björkman and C. P. Snapp, "Small-signal noise behavior of companion p$^+$-n-p$^+$ and p$^+$-n-ν-p$^+$ punchthrough microwave diodes," *Electron Lett.*, vol. 8, pp. 501–503, Oct. 1972.
[11] J. Helmcke, H. Herbst, M. Claassen, and W. Harth, "FM noise and bias-current fluctuations of a silicon Pd-n-p$^+$ microwave oscillator," *Electron Lett.*, vol. 8, pp. 158–159, Mar. 1972.
[12] H. Herbst and W. Harth, "Frequency modulation sensitivity and frequency pushing factor of a Pd-n-p$^+$ punchthrough microwave diode," *Electron Lett.*, vol. 8, pp. 358–359, July 1972.
[13] W. A. Edson, "Noise in oscillators," *Proc. IRE*, vol. 48, pp. 1454–1466, Aug. 1960.
[14] K. Kurokawa, "Some basic characteristics of broadband negative resistance oscillator circuits," *Bell Syst. Tech. J.*, vol. 48, pp. 1937–1955, July 1969.
[15] J. L. Fikart and P. A. Goud, "The direct-detection noise-measuring system and its threshold," *IEEE Trans. Instrum. Meas.*, vol. IM-21, pp. 219–224, Aug. 1972.
[16] J. R. Ashley, C. B. Searles, and F. M. Palka, "The measurement of oscillator noise at microwave frequencies," *IEEE Trans. Microwave Theory Tech. (Special Issue on Noise)*, vol. MTT-16, pp. 753–760, Sept. 1968.
[17] P. A. Levine, H. C. Huang, and H. Johnson, "IMPATTs shoot for Gunn noise levels," *Microwaves*, pp. 52–56, Apr. 1972.
[18] D. B. Leeson, "Short term stable microwave sources," *Microwave J.*, vol. 13, pp. 59–69, June 1970.
[19] M. El-Gabaly, J. Nigrin, and P. A. Goud, "Stationary charge transport in metal-semiconductor-metal (MSM) structures," *J. Appl. Phys.*, to be published.
[20] Raytheon Company, "60 GHz line of sight microwave link," *Microwave J.*, vol. 12, p. 38, Nov. 1969.

New Theory and Design for Hairpin-Line Filters

ULRICH H. GYSEL, MEMBER, IEEE

Abstract—**Hairpin-line and hybrid hairpin-line/half-wave parallel-coupled-line filters are preferred filters for microstrip and TEM printed-circuit realizations. This class of filters offers small size and, in general, needs no ground connections for resonators.**

A new design theory is presented that is based on a sparse capacitance matrix for the array of coupled lines that constitute the filter, as opposed to a sparse-inductance-matrix assumption in previous theories that is much harder to satisfy. It is shown that to a good approximation, hairpin-line filters result from frequency-scaling half-wave parallel-coupled-line filters. Because of this, the bandwidth can be accurately predicted.

Design procedures are given for Type-*A* filters, which are useful up to 20-percent bandwidth. A variety of hybrid hairpin-line/half-wave parallel-coupled-line filters is possible, and their design is explained. Numerical results for a number of designs and experimental results for a 5-percent bandwidth filter are included.

I. INTRODUCTION

THE hairpin-line filter, like the half-wave parallel-coupled-line filter, is one of the preferred configurations in stripline or microstrip because ground connections are not required. Basically, the hairpin-line filter can be thought of as a folded version of a half-wave parallel-coupled-line filter. The hairpin-line filter makes a much more compact filter than the half-wave parallel-coupled-line filter, but is expected to have much the same performance. However, the additional coupling between the two lines that constitute a hairpin resonator complicates the design.

The image parameters for the infinite periodic hairpin line have been reported by Bolljahn and Matthaei [1]. Only recently, design equations have been given for finite length hairpin-line filters by Cristal and Frankel [2]. Their design theory is based on the assumption of a sparse *inductance* matrix for the array of coupled lines. But for most parallel-coupled-line-type filters, the assumption of a sparse *capacitance* matrix is made. This, as Cristal and Frankel [2] state, corresponds much more closely to the physical reality than does neglecting inductive coupling beyond nearest neighbors. Further, this design theory [2] needs an empirically determined bandwidth contraction factor, depending on the hairpin resonator coupling.

The present paper gives exact equivalent circuits for odd-order hairpin-line filters of Types *A* and *B* that are based on a sparse capacitance matrix. This leads to designs that are exact for any practical purposes up to 20-percent bandwidth for Type-*A* filters and up to 50-percent bandwidth for Type-*B* filters. In particular, the bandwidth can be predicted accurately. From a theoretical point of view, it is most interesting that the new design method explains the bandwidth contraction factor in [2] and particularly shows that it is independent of the number of resonators, of passband ripple, and, largely, of bandwidth. This is the

Manuscript received May 2, 1973; revised November 30, 1973. This work was sponsored by a Postdoctoral Fellowship granted to the author by the Swiss National Science Foundation.

The author is with the Stanford Research Institute, Menlo Park, Calif. 94025.

primary contribution of the new theory. For the practical design of these filters, only a slight improvement over Cristal and Frankel's design [2] is achieved.

In most cases a hybrid hairpin-line/half-wave parallel-coupled-line filter will be preferred because a serious surface-wave-mode problem exists [2] in pure hairpin-line filters constructed in microstrip form. This mode can be prevented by the use of hybrid hairpin-line/half-wave parallel-coupled-line designs. A large variety of hybrid designs for any bandwidth can be readily developed by the method presented here. Hybrid even-order filters also can be designed with high accuracy.

The new design is based on the general n-wire line, as discussed by Matsumoto [3]. An n-port is created by looking into the n-ports at the input of an n-wire line that is terminated in an ideal transformer bank at the far end. For that n-port an equivalent circuit is developed. By neglecting insignificant terms, this circuit can be identified with a modified equivalent circuit of the half-wave parallel-coupled-line filter. The new theory has been verified with several trial designs and experimental results on a 5-percent-bandwidth filter are presented.

II. EQUIVALENT CIRCUITS FOR ODD-ORDER HAIRPIN-LINE FILTERS

A. The General n-Wire Line Representation

The general n-wire coupled-transmission line above a ground plane, shown in Fig. 1, may be described by the admittance equation:

$$\begin{bmatrix} i_1 \\ i_2 \\ \cdot \\ \cdot \\ \cdot \\ i_n \\ \cdot \\ \cdot \\ \cdot \\ i_{2n} \end{bmatrix} = \frac{1}{s} \begin{bmatrix} n \times n & n \times n \\ [C] & -t[C] \\ & \\ & \\ n \times n & n \times n \\ -t[C] & [C] \end{bmatrix} \begin{bmatrix} v_1 \\ v_2 \\ \cdot \\ \cdot \\ \cdot \\ v_n \\ \cdot \\ \cdot \\ \cdot \\ v_{2n} \end{bmatrix} \tag{1}$$

where

s	$= j \tan \beta l = j \tan (\pi f / 2 f_0)$;
β	propagation constant;
l	a commensurate length of the network;
t	$(1 - s^2)^{1/2}$; (2)
f	frequency variable of the commensurate network;
f_0	quarter-wave frequency of the commensurate network;
matrix $[C]$	static capacitance distribution for the coupled-line network normalized to $Y_n \rho^{-1}$, where Y_n is a normalization admittance and ρ is the velocity of light in the medium of propagation.

The elements of the matrix $[C]$ are defined by:

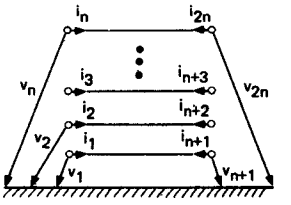

Fig. 1. General coupled n-wire line above a ground plane.

$$[C] = \begin{bmatrix} C_{11} & -C_{12} & -C_{13} & \cdots & \cdots \\ -C_{12} & C_{22} & -C_{23} & \cdots & \cdots \\ \cdots & -C_{23} & C_{33} & \cdots & \cdots \\ \cdot & \cdot & \cdot & & \\ \cdot & \cdot & \cdot & & \\ \cdot & \cdot & \cdot & \cdots & C_{nn} \end{bmatrix} \tag{3}$$

where

$$\begin{aligned} C_{ij} &= C_{ji} \\ C_{ij} &\geq 0 \\ C_{ii} &\geq \sum_{j \neq i} C_{ij}, \qquad \text{for } i = 1,2,\cdots,n \end{aligned} \tag{4}$$

It is convenient to assign separate voltage and current vectors to the two different sides of the n-wire line, called primary side and secondary side, respectively:

$$\begin{aligned} [I_1] &= [i_1, i_2, \cdots, i_n]^T \\ [I_2] &= [i_{n+1}, i_{n+2}, \cdots, i_{2n}]^T \\ [V_1] &= [v_1, v_2, \cdots, v_n]^T \\ [V_2] &= [v_{n+1}, v_{n+2}, \cdots, v_{2n}]^T. \end{aligned} \tag{5}$$[1]

A compact form of (1) therefore reads:

$$\begin{bmatrix} I_1 \\ I_2 \end{bmatrix} = \frac{1}{s} \begin{bmatrix} [C] & -t[C] \\ -t[C] & [C] \end{bmatrix} \begin{bmatrix} V_1 \\ V_2 \end{bmatrix}. \tag{6}$$

Hairpin-line filters can be visualized as n wire lines with interconnections on both sides. Fig. 2 shows hairpin-line filters of Types A and B, both of odd order. To derive their equivalent circuit we follow a procedure described by Matsumoto [3, ch. 8]. The interconnections on both sides of the n-wire line are made with ideal transformer banks. Let us terminate the secondary side by the transformer bank T_2. Then the transformed variables are defined as follows:

$$[I_2'] = [T_2][I_2] \tag{7}$$

and

$$[V_2] = [T_2]^T [V_2'] \tag{8}$$

with $[T_2]$ a $n_2 \times n$ matrix.

The case of a hairpin-line filter of Type A, together with the appropriate form of $[T_2]$, is shown in Fig. 3. Sub-

[1] T denotes the transposed matrix or vector.

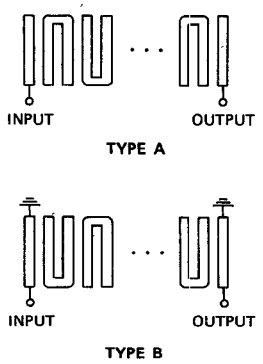

Fig. 2. Hairpin-line filters.

stituting (8) into the second row of (6) and multiplying both sides by $[T_2]$ from the left gives

$$[I_2'] = [T_2][I_2] = -\frac{t}{s}[T_2][C][V_1] + \frac{1}{s}[T_2][C][T_2]^T[V_2']. \quad (9)$$

However, $[I_2'] = [0]$, as can be seen from Fig. 3. We solve (9) for $[V_2']$ and substitute this into the first row of (6). With the notation

$$[\tilde{C}] = [T_2][C][T_2]^T \quad (10)$$

this yields

$$[I_1] = \left\{\frac{1}{s}[C] - \frac{t^2}{s}[C][T_2]^T[\tilde{C}]^{-1}[T_2][C]\right\}[V_1]. \quad (11)$$

Recognizing that $t^2 = 1 - s^2$, we can write this as

$$[I_1] = \left\{\frac{1}{s}[C_L] + s[C_C]\right\}[V_1] \quad (12)$$

where

$$[C_C] = [C][T_2]^T[\tilde{C}]^{-1}[T_2][C] \quad (13)$$

$$[C_L] = [C] - [C_C]. \quad (14)$$

If some lines on the primary side are interconnected, we proceed in a similar way with a transformer bank T_1, which is given by

$$[I_1'] = [T_1][I_1]$$
$$[V_1] = [T_1]^T[V_1'] \quad (15)$$

where $[T_1]$ is an $m_1 \times n$ matrix.

Substituting (15) into (12) results in

$$[I_1'] = [T_1]\left\{\frac{1}{s}[C_L] + s[C_C]\right\}[T_1]^T[V_1']. \quad (16)$$

Now, for the example of Fig. 3, we have to impose the condition $i_4' = 0$. This requires the hairpin resonator that is formed by connecting nodes 4 and 5 on the primary side[2] to operate essentially in an odd mode as long as only the admittance matrix of the n-wire line without terminations is considered. The odd mode of operation is forced by changing the voltage reference of lines 5–8 and then equating v_4 to $-v_5$. The transformer network $[T_1]$ is also shown in Fig. 3. With the notation

$$[C_L'] = [T_1][C_L][T_1]^T$$
$$[C_C'] = [T_1][C_C][T_1]^T \quad (17)$$

(16) can be written as

$$[I_1'] = \left\{\frac{1}{s}[C_L'] + s[C_C']\right\}[V_1'] \quad (18)$$

and

$$[C_L'] + [C_C'] = [T_1][C][T_1]^T = [C']. \quad (19)$$

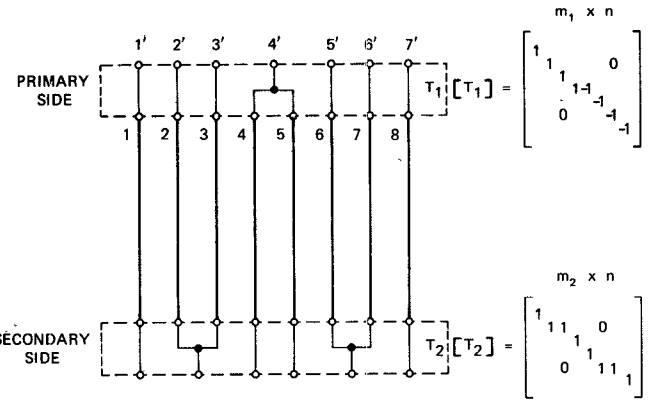

Fig. 3. n-wire line and transformer banks to form a hairpin-line filter of Type A ($n = 8$).

B. The Equivalent Circuit

To find an equivalent circuit for the odd-order hairpin-line filter of Type A, we notice that (12) and (18) represent a parallel connection of two n and m_1 ports, respectively, one purely inductive, and the other purely capacitive. Fig. 4(a) shows the equivalent circuit corresponding to (12). Since a Type-A hairpin-line filter has no lines connected to ground, no grounded inductor can appear in the equivalent circuit. Series inductors exist between those primary side ports that show a dc path between them due to an interconnection on the secondary side. All inductors are coupled to each other and, to satisfy (14), these inductive couplings are accompanied by capacitive couplings of the same amount, which can be seen as follows. We recall that $[C]$ is assumed to be a sparse matrix. If we denote the elements of $[C_L]$ and $[C_C]$ by γ_{ij} and δ_{ij}, respectively, then (14) can be written as

$$\gamma_{ij} + \delta_{ij} = \begin{cases} C_{ii}, & j = i \\ -C_{ij}, & j = i \pm 1 \\ 0, & j \neq i, i \pm 1 \end{cases} \quad (20)$$

[2] Throughout the rest of the paper such hairpin resonators will be simply called primary-side resonators. In the same way, hairpin resonators folded on the secondary side and with their open-circuited ends on the primary side are called secondary-side resonators.

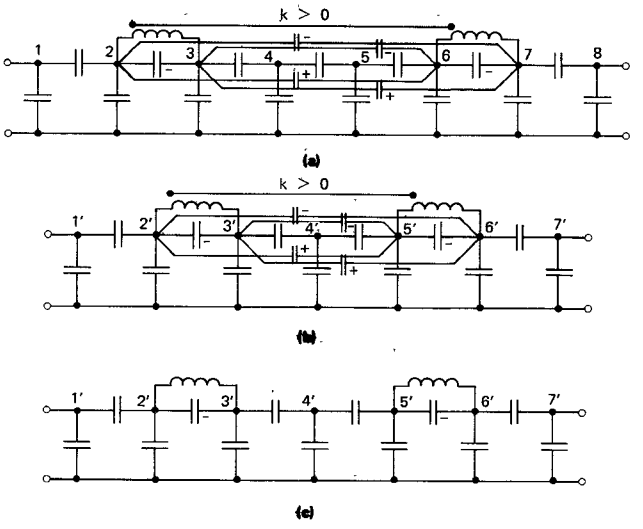

Fig. 4. Equivalent circuit of the Type-A hairpin-line filter ($n = 8$). (a) Without transformer bank T_1. (b) Complete equivalent circuit. (c) Simplified equivalent circuit.

or $|\ \gamma_{ij}\ | = |\ \delta_{ij}\ |$, for all $j \neq i$, $i \pm 1$, which holds for all inductive couplings.

The effect of the transformer $[T_1]$, which is not yet included in the circuit of Fig. 4(a), is to combine nodes 4 and 5 in one single node 4'. This leads to the final exact equivalent circuit of Fig. 4(b). Due to the form of $[T_1]$, the transformation (19) results also in a sparse $[C']$ matrix, and thus an equation analogous to (20) could be written down for the elements of $[C_L']$ and $[C_C']$.

The numerous capacitive and inductive coupling elements beyond immediate neighbors in Fig. 4(a) and (b) decrease rapidly the more lines they cross. If we define coupling factors of the $[C]$ matrix by

$$C_p = \frac{C_{ij}}{(C_{ii}C_{jj})^{1/2}}, \qquad j = i + 1 \tag{21a}$$

or, in decibels,

$$c_p = -20 \log_{10} C_p \tag{21b}$$

then the coupling elements between two nonadjacent lines having, say, r lines between them is on the order of C_p^{r+1}. This was verified numerically in a number of cases. For many practical hairpin-line filters these coupling elements are so small (e.g., less than 1/50 of the mutual coupling in the original array) that they can be safely neglected. This leads to a simplified equivalent circuit as shown in Fig. 4(c).

Finally, we will examine the zeros of the parallel-tuned circuits that exist between ports 2' and 3', and ports 5' and 6'. If γ_{ij}' and δ_{ij}' denote the elements of $[C_L']$ and $[C_C']$, respectively, the passivity of the circuit requires $\gamma_{i,i+1}' < 0$, $i = 2,5$ (positive inductors). A detailed analysis of (13) and (18) shows that $\delta_{i,i+1}' > 0$, $i = 2,5$, indicating a negative capacitor. Hence, these series branches create a transmission zero:

$$\sigma_{i,i+1} = (-\gamma_{i,i+1}'/\delta_{i,i+1}')^{1/2} \geq 1, \qquad i = 2,5. \tag{22}$$

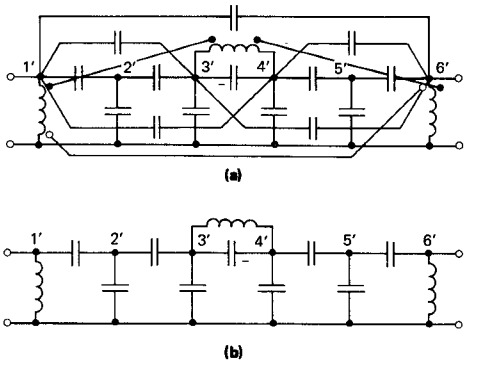

Fig. 5. Equivalent circuit of the Type-B hairpin-line filter ($n = 8$). (a) Complete circuit. (b) Simplified circuit.

Equation (22) holds with an equal sign for $C_{i,i+1}' = 0$. The physical reason for this real transmission zero becomes obvious if we look into the n-wire line from ports 2' and 3'. From these ports a secondary-side hairpin resonator looks essentially like a microwave C section. The latter has a real transmission zero $\sigma \geq 1$. Actually, the π-network present in Fig. 4(c) between ports 2' and 3' is one possible form for an equivalent circuit of a C section.

The procedure used to develop the equivalent circuit for Type-B filters is analogous to that for Type A. The only difference is the form of the transformer banks $[T_1]$ and $[T_2]$. Fig. 5 gives the complete and the simplified circuit for such a filter consisting of $n = 8$ lines.

The analysis presented in this section works well as long as input and output are on the same side of the n-wire line. This is the case for all odd-order filters. For even-order filters, if the input is on the primary side, then the output is on the secondary side. The output is therefore no longer an accessible port in an equivalent circuit of the form of either Fig. 4 or Fig. 5. A method to handle those cases is presented in the next section, together with the design procedure for odd-order filters.

III. DESIGN PROCEDURES FOR HAIRPIN-LINE FILTERS

In this paper, design procedures only for Type-A filters are developed. For the design of hairpin-line filters, it is most helpful to remember the close relationship between these filters and the half-wave parallel-coupled-line filters. In the limiting case, a hairpin-line filter with no coupling between the lines constituting hairpin resonators (hereafter simply called hairpin coupling) must be identical with a half-wave parallel-coupled-line filter. Therefore, the equivalent circuit of the hairpin-line filter, shown in Fig. 6(a), must be equivalent to the circuit of Fig. 4(b).

A. The Design Procedure

Networks containing unit elements like those shown in Fig. 6(a) cannot be frequency scaled in general (see e.g., Wenzel [4]). What can be scaled in frequency is the cascade connection of two unit elements, which can be represented differently by means of lumped equivalent circuits. One such representation is a π network containing a series

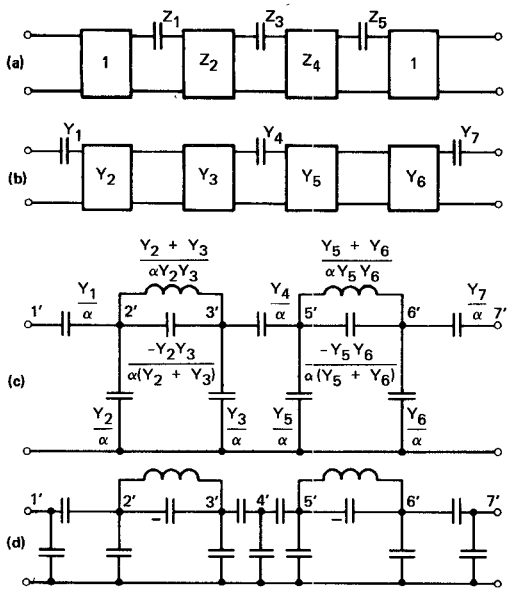

Fig. 6. Development of hairpin-line filters.

branch with a parallel-tuned circuit that creates the real transmission zeros at $s = \pm 1$ (the series C is negative). When this circuit is scaled by $f' = \alpha f$, the new circuit can be realized as a microwave C section [4].

The effect in this simple case is the introduction of coupling between two formerly uncoupled lines. But introducing coupling between formerly uncoupled lines is exactly the process that leads from half-wave parallel-coupled-line filters to hairpin-line filters. Therefore, it must be possible to frequency scale any odd-order half-wave parallel-coupled-line filter and transform it into a hairpin-line filter. It actually is possible to do this. We will prove it by carrying out the transformation steps and showing that the final capacitance matrix of the n-wire line is hyperdominant.

First, we outline the design procedure steps, and then give a closed form for the capacitance matrix of the n-wire line. This can be immediately used to determine the physical dimensions of the filter. We start with the selection of an appropriate half-wave parallel-coupled-line filter of odd-order N, as depicted for $N = 3$ in Fig. 6(a). For narrow-band cases this circuit has to be augmented by unit elements at the input and output to give reasonable impedance levels in the interior of the filter. Element values for the capacitors and unit elements may be taken from Cristal [5] or Horton and Wenzel [6]. The latter contains extensive tables for element values of interdigital filters. Filters with short-circuited input lines are duals of half-wave parallel-coupled-line filters of Type A. Therefore, using these tables we have to interpret the table value as elastances of the capacitors and impedances of the unit elements.

Next, we remove the series capacitors between every other unit element, as indicated in Fig. 6(b). This can be done most conveniently by an elastance matrix transformation. By using the tables in [6], the tabulated values directly become the normalized elastances and impedances if divided by 7.54. By labeling them $Z_1, Z_2 \cdots$, we form the initial elastance matrix as given on the left side in the following:

$$\begin{array}{c} \\ \times n_1 \\ \\ \\ \times n_5 \end{array}$$

$$\begin{bmatrix} 1 & -1 & 0 & 0 & 0 \\ -1 & 1+Z_1+Z_2 & -Z_2 & 0 & 0 \\ 0 & -Z_2 & Z_2+Z_3+Z_4 & -Z_4 & 0 \\ 0 & 0 & -Z_4 & Z_4+Z_5+1 & -1 \\ 0 & 0 & 0 & -1 & 1 \end{bmatrix} \begin{array}{l} \\ \times n_1 \\ \\ \\ \times n_5 \end{array}$$

$$= \begin{bmatrix} \frac{1}{Y_1}+\frac{1}{Y_2} & -\frac{1}{Y_2} & 0 & 0 & 0 \\ -\frac{1}{Y_2} & \frac{1}{Y_2}+\frac{1}{Y_3} & -\frac{1}{Y_3} & 0 & 0 \\ 0 & -\frac{1}{Y_3} & \frac{1}{Y_3}+\frac{1}{Y_4}+\frac{1}{Y_5} & -\frac{1}{Y_5} & 0 \\ 0 & 0 & -\frac{1}{Y_5} & \frac{1}{Y_5}+\frac{1}{Y_6} & -\frac{1}{Y_6} \\ 0 & 0 & 0 & -\frac{1}{Y_6} & \frac{1}{Y_6}+\frac{1}{Y_7} \end{bmatrix}. \quad (23)$$

Then the even-numbered rows and columns are multiplied by

$$n_i = \frac{Z_{i-1} + Z_{i+1}}{Z_{i-1} + Z_i + Z_{i+1}}, \qquad i = 1,5 \tag{24}$$

where the n_i are determined from the condition of no self-elastance in the even-numbered loops ($Z_0 = Z_{N+3} = 1$). The result is the new elastance matrix corresponding to the circuit of Fig. 6(b). The elements of this matrix are already given in terms of the circuit of Fig. 6(b). Now we transform each cascade of two unit elements into its lumped equivalent circuit.[3] At this stage we have a completely lumped circuit that can be frequency-scaled by dividing each L and C by the frequency-scale factor α. Its value will be determined later. The scaled circuit is shown in Fig. 6(c). To arrive at a circuit like that in Fig. 4(c), we must split the series capacitors between the former unit element pairs into preferably equal parts and apply a capacitance matrix transformation so that all nodes become a finite ground capacitance. The result of this procedure is shown in Fig. 6(d).

From this circuit $[C_L']$ and $[C_C']$ can be written down by inspection. It remains to reverse the step that led from the circuit of Fig. 4(a) to that of Fig. 4(b), due to the transformer $[T_1]$. This step affected only $[C_C]$ and the elements of $[C_C]$ and $[C_C']$ pertaining to lines 4 and 5 are related by

$$\delta_{44}' = \delta_{44} - 2\delta_{45} + \delta_{55}. \tag{25}$$

Restoring lines 4 and 5 has to leave δ_{44}' unchanged, which can be done by the following procedure:

$$[C_C] = \begin{bmatrix} \ddots & & & & \\ & b\,\delta_{44}' + \delta_{45} & +\delta_{45} & & \\ & +\delta_{45} & (1-b)\delta_{44}' + \delta_{45} & & \\ & & & \ddots & \\ & & & & \ddots \end{bmatrix} \begin{matrix} \\ 4 \\ 5 \\ \\ \end{matrix} \qquad \begin{matrix} \\ 4 & 5 \\ \\ \\ \end{matrix} \tag{26}$$

where $0 < b < 1$ and $\delta_{45} \leq 0$. This can be verified by back substitution of (26) into (25). Finally, summation of $[C_L]$ and $[C_C]$ leads to $[C]$, which is given in terms of the element values of Fig. 6(b) in the following:

$$[C] = \frac{1}{\alpha}\begin{bmatrix} Y_1 & -Y_1 & 0 & 0 & 0 & 0 & 0 \\ -Y_1 & Y_1 + Y_2 + Y_{23} & -Y_{23} & 0 & 0 & 0 & 0 \\ 0 & -Y_{23} & Y_{23} + Y_3 + \frac{Y_4}{a} & -\frac{Y_4}{a} & 0 & 0 & 0 \\ 0 & 0 & -\frac{Y_4}{a} & \frac{Y_4}{a} - Y_{45} & -Y_{45} & 0 & 0 \\ 0 & 0 & 0 & -Y_{45} & -Y_{45} + \frac{Y_4}{1-a} & -\frac{Y_4}{1-a} & 0 \\ 0 & 0 & 0 & 0 & -\frac{Y_4}{1-a} & \frac{Y_4}{1-a} + Y_5 + Y_{56} & -Y_{56} \\ 0 & 0 & 0 & 0 & 0 & -Y_{56} & Y_{56} + Y_6 + Y_7 \quad -Y_7 \\ 0 & 0 & 0 & 0 & 0 & 0 & -Y_7 \qquad Y_7 \end{bmatrix} \tag{27}$$

where

$$Y_{23} = (\alpha^2 - 1)\frac{Y_2 Y_3}{Y_2 + Y_3}$$

$$Y_{45} = -\alpha\delta_{45}$$

$$Y_{56} = (\alpha^2 - 1)\frac{Y_5 Y_6}{Y_5 + Y_6}.$$

Actually, the capacitance matrix transformation that turns all ground capacitances finite and positive remains to be done, which requires some precautions. If we want to change the admittance level of line k, $k = 2, 4, 6$, by an amount n_k, line $k + 1$ has to be changed by the same amount because those line pairs are dc connected and

[3] In the transformed or prototype variable.

cannot be changed independently. The factor a is preferably chosen as 1/2 to split Y_4 in half.

B. Proof of the Hyperdominance of [C]

It remains to show the hyperdominance of the final capacitance matrix [C] and to determine the frequency scale factor α as well as Y_{45}. This will be done for the design example, however, generalization is straightforward. First, we notice that all Y_i in Fig. 6(b) are positive. By definition the main-diagonal elements of [C] must be positive and all off-diagonal elements must be negative. This requires $\alpha \geq 1$ and $Y_{45} \geq 0$. The hyperdominance condition is fulfilled for $Y_{45} = 0$. If $Y_{45} > 0$, we raise the admittance level of nodes 4 and 5 by an amount n_4^2. Writing down the hyperdominance condition for the two nodes we get the condition

$$(n_4 - 1)\frac{Y_4}{a} - 2Y_{45} \geq 0, \qquad a \leq 0.5. \tag{28}$$

This can be fulfilled for any $Y_4 > 0$ and an $n_4 > 1$ with a sufficiently small Y_{45}. If $a > 0.5$, it has to be replaced by $(1 - a)$ in (28). In practice, this condition is very easy to satisfy. This proves the hyperdominance of the matrix [C].

The fact of $\alpha \geq 1$ indicates that the hairpin-line filter will always have a narrower bandwidth than its corresponding half-wave parallel-coupled-line counterpart. The bandwidth contraction depends on the amount of coupling. From (27) we calculate the coupling factor of the secondary-side hairpin resonators. After a slight simplification we get

$$C_p \approx \frac{\alpha^2 - 1}{\alpha^2 + 1}. \tag{29}$$

This formula slightly overestimates the coupling, but it serves as a guideline to select a bandwidth scale factor for a desired hairpin coupling. In practice, a coupling factor less than 10 dB is impractical and unnecessarily strong. In most cases, $\alpha = 1.1$ to 1.2 ($c_p = 20$ to 15 dB) is adequate.

The frequency scaling by α is performed on the lumped prototype variable s. To find the proper scaling of the real frequency variable f, we have to make use of the transformation given in (2). If w denotes the fractional bandwidth of the unscaled filter and w' the same for the scaled—i.e., the hairpin-line filter—the following relationship holds:

$$w = \frac{4}{\pi}\tan^{-1}\left\{\alpha \tan\frac{\pi w'}{4}\right\}. \tag{30}$$

For $w \leq 0.3$, a good approximation for this equation is

$$w = \alpha w'. \tag{31}$$

In general, w' is given and on selection of an appropriate α the fractional bandwidth for the unscaled half-wave parallel-coupled-line filter is determined.

The value for Y_{45} is normally selected to give about the same coupling value c_p as for secondary-side resonators ($a = 0.5$ assumed)

$$Y_{45} = \frac{2Y_4 C_p}{1 + C_p} \tag{32}$$

but any other reasonable value is possible.

C. Hybrid Forms

Unequal coupling for primary-side resonators can be used throughout the filter. This is in contrast to the coupling of secondary-side hairpin resonators that is fixed for all resonators as soon as α is chosen. By making $Y_{k,k+1} = 0$, $k = 4,8,\cdots$, a number of hybrid forms as shown in Fig. 7(a) and (b) can be created. These hybrid forms interrupt the surface-wave mode as shown in [2], and in most cases will be preferred over an all-hairpin design, even though they do not offer the optimum in space saving. In addition, the full hybrid form shown in Fig. 7(a) makes all coupling elements between nonadjacent nodes in Fig. 4(b) zero, so that the equivalent circuit of Fig. 4(c) is exact. As pointed out above, even-order half-wave parallel-coupled-line filters cannot be scaled in frequency because they contain an odd number of unit elements. However, a hybrid form that leaves $\alpha = 1$ but introduces coupling between primary-side resonators is possible, as indicated in Fig. 6(c). To design such a filter the best way to start is to find the capacitance matrix of the half-wave parallel-coupled-line filter in the usual way, and then introduce coupling between primary-side resonators as previously indicated.

In the next section we will give experimental and numerical results. In particular, we must test the validity of the simplifications that led to the circuit of Fig. 4(c) and that eventually allowed us to design the filter.

IV. NUMERICAL AND EXPERIMENTAL RESULTS

The validity of the new design theory was checked by a number of trial designs. The main reason for this was to determine the extent to which the coupling elements beyond adjacent nodes can be safely neglected. The designs of the underlying half-wave parallel-coupled-line filter were taken from the table values [6]. The design equations (23) and (27) are easily programmed on a computer and give the capacitance matrix of the n-wire line network.

A. Numerical Results

Any check of the actual response of the filter has to be done by means of an exact equivalent circuit. The graph transformation method by Sato and Cristal [7] was used for this purpose because it is easier to use than the exact equivalent circuit of Fig. 4(b). All filters designed and analyzed had a ripple of 0.1 dB. They were checked for fractional bandwidths $w = 0.05$, 0.1, and 0.2. For odd-

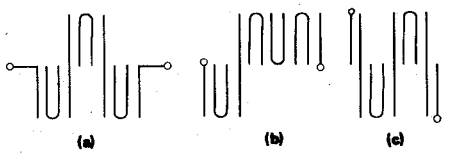

Fig. 7. Hybrid forms of hairpin-line/half-wave parallel-coupled-line filters. (a) and (b) $\alpha \neq 1$. (c) $\alpha = 1$.

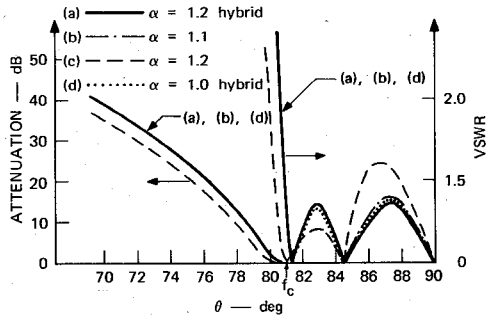

Fig. 8. Computed response for Type-A hairpin-line filters using exact equivalent circuits ($N = 5$, $w = 0.2$).

order filters with $w = 0.05$, no deviation of the response from the theoretical was discovered up to $\alpha = 1.2$ (corresponding to 15-dB hairpin coupling). At 10-percent bandwidth a slight change in the VSWR in the passband was noticed for $\alpha = 1.2$. The results for filters of order $N = 5$ and $w = 0.2$ are shown in Fig. 8. Curve (a) is the response of the hybrid form with no hairpin coupling between primary-side resonators [Fig. 7(a)] and $\alpha = 1.2$. This response is exact, as was pointed out above. For the full hairpin-line filter with $\alpha = 1.1$, very small deviations in the passband are visible, whereas for $\alpha = 1.2$ [curve (c)] the maximum VSWR has increased to 1.6 and the bandwidth is slightly larger than predicted. Curve (d) is the case of a hybrid filter with $\alpha = 1$—i.e., no hairpin coupling between secondary-side resonators [see Fig. 7(c)]. The deviations for this filter are very minor also. In all cases except one, the desired bandwidth was virtually exact. To minimize the deviations from the theoretical response, α should not exceed a value that depends on the bandwidth of the filter. As a guideline, take $\alpha \leq 1.2$ for $w \leq 0.1$, which should be decreased to $\alpha \leq 1.12$ for $w = 0.2$. An even-order filter ($N = 4$) of hybrid form with $\alpha = 1$ and a hairpin coupling of 14 dB was also tested and found to agree very closely with the theoretical response.

B. Experimental Results

A practical stripline version was built and tested. It is a hybrid filter of the form of Fig. 7(a) with $N = 5$, $w = 0.05$, $\alpha = 1.1$, and 0.1-dB ripple, as shown in Fig. 9. The printed-circuit construction was made on 0.125-in (0.3175-cm) Tellite material ($\epsilon_r = 2.32$); hence the total ground-plan spacing was 0.25 in (0.635 cm). The nominal center frequency of the filter is 1.5 GHz. The measured attenuation and return loss are shown in Fig. 10. The VSWR in the passband was equal to or below 1.36, the theoretical value,

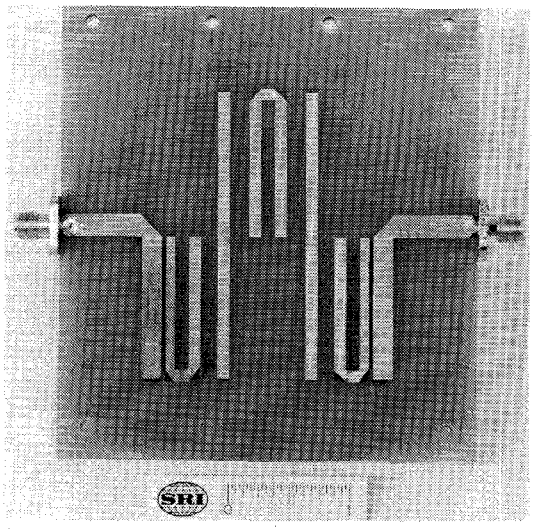

Fig. 9. Hybrid hairpin-line/half-wave parallel-coupled-line filter ($N = 5$, $w = 0.05$).

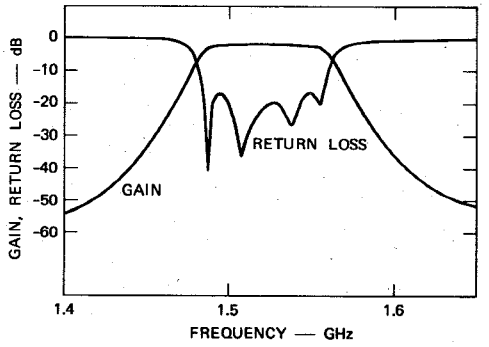

Fig. 10. Measured return loss and attenuation for trial hybrid filter ($N = 5$, $w = 0.05$).

and the bandwidth as measured between the 16.5-dB return loss points is approximately 0.049. Both VSWR and bandwidth are in very good agreement with theory. The stopband was free of any spurious responses to −50 dB at all frequencies up to the next passband at 4.5 GHz. A second similar filter with a bandwidth of 0.1 and a center frequency of 1.6 GHz gave nearly as good results. It showed a bandwidth contraction of 5 percent that is attributed to the discontinuity reactances that are inevitable at the bend of the hairpin resonators.

V. SUMMARY AND CONCLUSIONS

A new theory for hairpin-line and hybrid hairpin-line/half-wave parallel-coupled-line filters has been presented, and explicit design equations have been given. The new theory gives a better understanding of the process that leads to bandwidth contraction as the resonators of a half-wave parallel-coupled-line filter are folded to form hairpin resonators. This process is accompanied by a frequency scaling of the filter response so that a smaller passband results. Based on this theory, new design procedures have been developed that allow a rapid computa-

tion of hairpin-line filters and a variety of hybrid structures. For bandwidths up to 0.1, the procedure is virtually exact for any reasonable hairpin coupling. For larger bandwidth, the effect of the hairpin coupling on the frequency response should be checked.

In all cases, the VSWR was found to deteriorate long before any significant change in bandwidth was noted. The design applies to odd-order filters only, but this is not a serious restriction. In many cases a hybrid realization is preferred. But a very satisfactory hybrid design for even-order filters is presented.

The new design theory slightly improves the agreement of computed and theoretical response if compared with a design of comparable hairpin coupling given by Cristal and Frankel [2]. But more important is the theoretical explanation the new theory provides for the bandwidth contraction factor introduced in [2]. The relative bandwidth contraction as a function of c_p given in [2] was found to be in close agreement with (29). In their experiments, Cristal and Frankel found an even larger bandwidth contraction that they attributed to the finite-length connections between pairs of lines constituting a hairpin resonator. Such additional contraction was also found in the present experiments. Finally, it should be noted that the amount of bandwidth contraction for hybrid designs following the process in [2] is not precisely known. In contrast, our new design theory gives exact information about possible hybrid forms and about the parameters that control them.

ACKNOWLEDGMENT

The author wishes to thank Dr. L. Young and Dr. E. G. Cristal, both formerly with Stanford Research Institute, for their helpful discussions on this topic.

REFERENCES

[1] J. T. Bolljahn and G. L. Matthaei, "A study of the phase and filter properties of arrays of parallel conductors between ground planes," *Proc. IRE*, vol. 50, pp. 299–311, Mar. 1962.
[2] E. G. Cristal and S. Frankel, "Hairpin-line and hybrid hairpin-line/half-wave parallel-coupled-line filters," *IEEE Trans. Microwave Theory Tech.*, vol. MTT-20, pp. 719–728, Nov. 1972.
[3] A. Matsumoto, Ed., *Microwave Filters and Circuits, Supplement 1 to Advances in Microwaves*. New York: Academic, 1970.
[4] R. J. Wenzel, "Small elliptic-function low-pass filters and other applications of microwave C sections," *IEEE Trans. Microwave Theory Tech. (1971 Symposium Issue)*, vol. MTT-18, pp. 1150–1158, Dec. 1970.
[5] E. G. Cristal, "New design equations for a class of microwave filters," *IEEE Trans. Microwave Theory Tech.* (Corresp.), vol. MTT-19, pp. 486–490, May 1971.
[6] R. J. Wenzel and M. C. Horton, "Exact design techniques for microwave filters," Bendix Res. Lab., Southfield, Mich., Final Rep., Contract DA28-043-AMC-00399(e), Feb. 1–Apr. 30, 1965.
[7] R. Sato and E. G. Cristal, "Simplified analysis of coupled transmission-line networks," *IEEE Trans. Microwave Theory Tech.*, vol. MTT-18, pp. 122–131, Mar. 1970.

Holographic Imaging with Object Synthesized Apertures

NABIL H. FARHAT, SENIOR MEMBER, IEEE, AND PETER C. WANG

Abstract—**A method for imaging remote moving objects with a giant thinned holographic array by monitoring the range and range-rate (Doppler) histories of a coherently illuminated object at the various elements of the array is discussed. Electrooptic processing and image retrieval from the raw data collected are described together with a technique that compensates for image distortion arising from irrotational object maneuvers. Results of confirming experiments are also given together with remarks on practical implementation.**

Manuscript received September 12, 1973; revised December 26, 1973.

N. H. Farhat is with the Moore School of Electrical Engineering, University of Pennsylvania, Philadelphia, Pa. 19174.
P. C. Wang is with Department F97, IBM Corporation, San Jose, Calif. 95144.

I. INTRODUCTION

AN OBVIOUS variation of the conventional synthetic aperture radar [1] is one in which the imaging aperture is synthesized by object motion within the beam of a stationary coherent transmitter–receiver complex. An early account of such an imaging concept employing radio waves was given by Rogers [2] in an attempt to extend Gabor's diffraction microscopy (holography) [3] to the imaging of moving ionospheric regions. More recently, infrared and optical imaging apertures synthesized by linear object motion were discussed [4],[5]. In these studies uniformity of object motion was assumed and maintained to avoid image distortion arising